Photonic and Quantum Waves
https://www.sciltp.com/journals/pqw

Article

Dissipative Dynamics and Active Stabilization of Linear and Nonlinear Waves in Non-PT-Symmetric Harmonic Traps

Mario Salerno

Dipartimento di Fisica “E.R. Caianiello”, and INFN Sezione di Napoli-Gruppo Collegato di Salerno, Università di Salerno, Via Giovanni Paolo II, 84084 Fisciano, Italy; salerno@sa.infn.it

How To Cite: Salerno, M. Dissipative Dynamics and Active Stabilization of Linear and Nonlinear Waves in Non-PT-Symmetric Harmonic Traps. *Photonic and Quantum Waves* **2026**, *1*(1), 5.

Received: 12 May 2026
Revised: 9 August 2026
Accepted: 18 August 2026
Published: 24 August 2026

Abstract: We investigate the dissipative dynamics of linear and nonlinear waves in harmonic traps by means of engineered complex non-Hermitian potentials. By combining an analytical mapping between real and complex Schrödinger equations with direct numerical simulations, we show that while in the linear case the damped motion leads to the formation of a stationary state at the trap center, in the nonlinear case a static potential design alone is insufficient to ensure long-term stability. Instead, the system relaxes toward a long-lived metastable configuration that eventually undergoes decay or collapse. To overcome this limitation, we introduce a time-dependent modulation of the nonlinearity that effectively converts these metastable states into robust non-equilibrium stationary states. This approach establishes a general strategy for controlling nonlinear waves in non-Hermitian systems, with potential applications in photonics and Bose–Einstein condensates.

Keywords: non-PT-symmetric potentials; non equilibriun stationary states; nonlinear management; linear and nonlinear waves

1. Introduction

The study of dissipative wave phenomena in nonlinear media with complex parameters has become a central topic in modern physics [1,2]. Such systems arise naturally in a wide range of contexts, from the optics of active media, such as laser cavities and amplifying fibers [3,4], to quantum systems with effective non-Hermitian dynamics describing interactions with an environment [5,6]. In recent years, particular attention has been devoted to nonlinear wave propagation in complex potentials, motivated by advances in matter waves in dissipative optical lattices [7–10] and by the rapid development of non-Hermitian photonics [11,12].

A major breakthrough in this field was the introduction of $\mathcal{PT}$-symmetric potentials, which are invariant under the combined action of parity ($\mathcal{P}$) and time-reversal ($\mathcal{T}$) symmetry [13,14]. These systems, extensively investigated theoretically [15,16] and experimentally realized in optical settings [17,18], can exhibit entirely real spectra despite the presence of gain and loss.

While the linear properties of $\mathcal{PT}$-symmetric systems, including phase transitions and exceptional points [19], are now well understood, the nonlinear regime remains comparatively less explored. In particular, although stationary localized and periodic states exist in $\mathcal{PT}$-symmetric media [20–23], their stability and dynamical robustness remain open issues.

Recent studies have also revealed intriguing topological phenomena in non-Hermitian systems, including non-Hermitian jumps, topological loops associated with exceptional-point encircling, and dressing-induced quantization in atomic and photonic platforms [24,25]. These phenomena originate from the topology of the non-Hermitian spectrum under adiabatic parameter evolution and exceptional-point encircling. By contrast, the present work addresses a different physical mechanism, namely the dissipative relaxation and stabilization of localized nonlinear waves through the spatial engineering of complex gain–loss potentials rather than through topological properties of the non-Hermitian spectrum.

Motivated by these developments, we address a complementary question: can non-equilibrium nonlinear stationary states with real energies exist even in the absence of symmetry? While symmetry plays a crucial role in ensuring real spectra in linear systems, nonlinear media may sustain localized states through a balance between dispersion, nonlinearity, and gain–loss mechanisms, even when the underlying potential is not $\mathcal{PT}$ symmetric [22,26].

A paradigmatic setting in which to address this problem is the dynamics of a localized wave in a harmonic trap. While linear wave packets can be damped to rest at the trap center, the required complex potential is not a simple imaginary gradient $i\gamma x$. Indeed, a $\mathcal{PT}$-symmetric potential of this form cannot damp the center-of-mass motion. Efficient damping requires, as we demonstrate below, a non-$\mathcal{PT}$-symmetric complex potential whose imaginary part combines an odd contribution with a quadratic term that explicitly breaks $\mathcal{PT}$ symmetry.

In this work, we address this problem by combining numerical simulations with an analytical construction based on a mapping between real and complex nonlinear Schrödinger equations [27]. This approach allows us to design static non-$\mathcal{PT}$-symmetric potentials that, in the linear case, reproduce the desired center-of-mass damping and lead to the formation of a non-equilibrium stationary state (NESS) [28].

In the nonlinear regime, however, the situation is fundamentally different. An initial condition displaced from equilibrium undergoes damped motion toward the trap center but does not relax to a truly stationary state. Instead, the dynamics leads to a long-lived metastable configuration whose eventual fate depends on the sign of the nonlinearity: decay in the repulsive case and collapse in the attractive one. This behavior reflects an imperfect balance between gain and loss at the trap center, which cannot be fully compensated by a static potential design alone.

To stabilize the relaxed state at the center of the trap, we introduce a time-dependent nonlinear management (NM) protocol [29] that dynamically modulates the interaction strength as the wave approaches the metastable regime. This active control suppresses the residual gain–loss imbalance, transforming the metastable configuration into a robust NESS.

To the best of our knowledge, this work provides the first evidence that controlled damping of nonlinear waves toward a stationary state can be achieved by combining static non-$\mathcal{PT}$ complex potentials with active nonlinear control. These results are relevant for non-Hermitian photonics, where dissipative solitons must be stabilized in the presence of gain and loss [2], and for Bose–Einstein condensates, where Feshbach resonance techniques allow precise tuning of interatomic interactions [30].

The paper is organized as follows. In Section 2, we introduce the model equations and the mapping between real and complex NLS equations. In Section 3, we apply the method to the linear harmonic oscillator, where the mapping yields exact dissipative dynamics. In Section 4, we extend the analysis to the nonlinear regime, considering both repulsive and attractive interactions. In Section 5, we demonstrate the stabilization of metastable states via nonlinear management. Finally, Section 6 summarizes our conclusions and briefly discusses possible experimental perspectives.

2. Model Equations and Mapping between Real and Complex NLS

The dynamics of nonlinear waves in non-Hermitian media is described by the normalized nonlinear Schrödinger (NLS) equation:

$$i\psi_t = -\frac{1}{2}\psi_{xx} + \mathcal{V}(x)\psi + \sigma|\psi|^2\psi, \tag{1}$$

where the complex potential $\mathcal{V}(x)$ accounts for linear gain and loss:

$$\mathcal{V}(x) = V(x) + iW(x), \tag{2}$$

with $V(x)$ and $W(x)$ being real functions. The imaginary part $W(x)$ represents a spatially distributed gain–loss landscape through which the wave continuously exchanges energy (or, in Bose–Einstein condensates, particles) with the surrounding medium. Its specific spatial profile determines whether the gain–loss balance merely sustains a stationary state or actively drives dissipative dynamics. As will be shown below, a purely odd ($\mathcal{PT}$-symmetric) distribution is insufficient to damp the center-of-mass motion, whereas the addition of an quadratic contribution breaks the $\mathcal{PT}$ symmetry and opens an effective dissipative channel leading to relaxation toward the trap center.

This model encompasses several physically relevant situations. In the linear limit, it describes quantum dissipative systems or light propagation in lossy waveguides. In the nonlinear regime, it corresponds to the Gross–Pitaevskii equation for Bose–Einstein condensates with particle exchange, or to light propagation in active photonic media.

We seek stationary solutions of the form:

$$\psi(x,t) = A(x)e^{i\theta(x)}e^{-i\omega t}, \tag{3}$$

where $A(x)$ and $\theta(x)$ are real functions. Substituting Equation (3) into Equation (1) yields:

$$\omega A + \frac{1}{2}A_{xx} - \sigma A^3 - \frac{1}{2}(\theta_x)^2 A - VA = 0, \tag{4}$$
$$\frac{1}{2}A\theta_{xx} + A_x\theta_x - WA = 0. \tag{5}$$

Equation (5) has the form of a continuity equation for the particle (or optical) current. Multiplying it by A, it can be written as:

$$\frac{1}{2}(\theta_x A^2)_x = WA^2 \equiv \frac{dF(x)}{dx}, \tag{6}$$

where $F(x)$ represents the cumulative gain–loss balance. Integration of Equation (6) gives:

$$\theta_x = 2\frac{F(x)}{A^2}, \tag{7}$$
$$W(x) = \frac{1}{A^2}\frac{dF}{dx}. \tag{8}$$

Substituting Equation (7) into Equation (4) yields a nonlinear eigenvalue problem for the amplitude:

$$\left\{-\frac{1}{2}\frac{d^2}{dx^2} + V(x) + \sigma A^2 + 2\left(\frac{F(x)}{A^2}\right)^2\right\} A = \omega A, \tag{9}$$

which is equivalent to the original complex NLS for stationary states.

The mapping becomes particularly useful when $F(x)$ is chosen as a functional of the density. In the simplest case, we take:

$$F(x) = \frac{1}{2}C_n A^{n+2}, \quad n = 0, 1, 2, \ldots, \tag{10}$$

where C_n is a real constant. Equation (9) then reduces to the real eigenvalue problem:

$$\left\{-\frac{1}{2}\frac{d^2}{dx^2} + V(x) + \sigma A^2 + \frac{C_n^2}{2}A^{2n}\right\} A = \omega A. \tag{11}$$

Once the amplitude $A(x)$ and eigenvalue ω are determined (analytically or numerically, e.g., via self-consistent methods [31]), the imaginary potential follows self-consistently from Equation (8).

Different choices of n correspond to different effective nonlinearities. For instance, $n = 1$ yields a cubic correction, while higher values generate higher-order nonlinear terms. These can be formally absorbed into a redefinition of the real potential:

$$V = \tilde{V} - \frac{C_n^2}{2}A^{2n}, \tag{12}$$

thus preserving the mapping structure. The approach can be extended to analytic functionals:

$$F(x) = \frac{1}{2}\sum_{n=0}^{k} C_n A^{n+2}, \tag{13}$$

as well as to spatial derivative expansions of the amplitude of the form:

$$F(x) = \sum_{n,m} C_{n,m}\frac{d^m A^{n+2}}{dx^m}. \tag{14}$$

The latter are particularly useful for modeling specific dynamical effects, such as the quadratic damping encountered in harmonic traps.

In all cases, the mapping guarantees that the resulting stationary solutions possess real eigenvalues (chemical potentials), despite the presence of complex potentials, ensuring their physical relevance in non-Hermitian photonics and dissipative quantum systems.

A related reverse-engineering approach was considered in Ref. [21], where exact periodic waves, solitons, and breathers of the NLS equation with complex potentials were constructed analytically.

In the following sections, we apply the method first to the linear damped harmonic oscillator and then to the nonlinear dissipative case in non-$\mathcal{PT}$-symmetric complex potentials. We emphasize, however, that the mapping is exact for stationary states, where the target profile satisfies the mapped eigenvalue problem by construction. Its extension to time-dependent problems should instead be regarded as a potential-design strategy. It becomes exact in the linear harmonic oscillator because the Gaussian wave packet preserves its functional form throughout the evolution, whereas in nonlinear systems the evolving profile generally departs from the stationary ansatz used in the potential construction, so that, in the absence of NM, only an approximate gain–loss balance can be achieved. This residual imbalance is precisely the origin of the long-lived metastable states discussed in Section 4 and motivates the nonlinear management protocol introduced in Section 5.

3. The Damped Linear Harmonic Oscillator

In this section, we consider the complex linear Schrödinger equation obtained from Equation (1) in the limit $\sigma = 0$. This case provides a fundamental benchmark for understanding dissipative dynamics in non-Hermitian systems.

We first restrict the mapping to the simplest choice, $n = 0$ in Equation (10), i.e., we take $F(x) = \frac{1}{2}C_0 A^2(x)$. The resulting real eigenvalue problem (11) reduces to a standard Schrödinger equation with a shifted eigenvalue $\omega = \Omega + C_0^2/2$. The corresponding imaginary potential and phase follow from the mapping as

$$W(x) = \frac{1}{A^2}\frac{dF}{dx} = C_0 \frac{A_x}{A}, \qquad \theta(x) = C_0 x. \tag{15}$$

Assuming that the NESS has the same functional form as the ground state of the harmonic oscillator, we take

$$A(x) = \left(\frac{\omega_0}{\pi}\right)^{1/4} e^{-\frac{\omega_0 x^2}{2}}, \tag{16}$$

which yields the imaginary potential

$$W(x) = C_0 \frac{A_x}{A} = -W_0 x, \qquad W_0 = C_0 \omega_0. \tag{17}$$

This configuration corresponds to a $\mathcal{PT}$-symmetric system, where gain ($x < 0$) and loss ($x > 0$) are spatially balanced. The associated stationary solution is

$$\psi(x,t) = A(x)\, e^{iW_0 x/\omega_0} e^{-i\omega t}. \tag{18}$$

This complex potential exactly supports the stationary state. However, despite its non-Hermitian character, it does not induce dissipative dynamics: a displaced initial wavefunction undergoes undamped oscillations. This reflects the unbroken $\mathcal{PT}$-symmetric phase, where the spectrum is real and no net dissipation occurs.

To describe genuinely damped dynamics, the mapping must be extended beyond the simple functional $F \propto A^2$. We therefore consider a functional that includes spatial derivatives (corresponding to $n = 0, m = 1$ in Equation (14)):

$$F(x) = a_1 A^2(x) + \frac{a_2}{2}\frac{d}{dx} A^2(x). \tag{19}$$

We choose the real potential as a shifted harmonic oscillator,

$$V(x) = \frac{1}{2}\Omega_0^2 x^2 + 4a_1 a_2 \omega_0 x, \tag{20}$$

with $\Omega_0^2 = \omega_0^2(1 - 4a_2^2)$. Under these conditions, the Gaussian profile (16) solves the real eigenvalue problem with eigenvalue

$$\omega = \frac{1}{2}(\omega_0 + 4a_1^2). \tag{21}$$

The corresponding imaginary potential and phase are

$$W(x) = \frac{1}{A^2}\frac{dF}{dx} = 2a_2\omega_0^2 x^2 - 2a_1\omega_0 x - a_2\omega_0, \tag{22}$$

$$\theta(x) = 2a_1 x - a_2 x^2. \tag{23}$$

In contrast to the $\mathcal{PT}$-symmetric case, the imaginary potential now includes a quadratic term ($\sim x^2$), which explicitly breaks $\mathcal{PT}$ symmetry and introduces a genuine dissipative channel. As shown in Figure 1c,d, a displaced initial state exhibits damped oscillations, with the center of mass approximately following

$$x_c(t) \sim x_0 e^{-\gamma t}. \tag{24}$$

At the same time, the peak density relaxes toward a stationary value, well described on average by

$$|\psi_c(t)|^2 \approx A_0 + \frac{e^{-\beta t} - 1}{\gamma}, \tag{25}$$

(red curve in Figure 1d), with $\beta = 0.08$, $\gamma = 15.1$, and A_0 the density amplitude of the undamped ground state ($A_0 \approx 0.5642$).

It is remarkable that, in the linear case, the mapping provides a systematic framework for engineering complex potentials that accurately reproduce the dynamics of a damped quantum oscillator. In this sense, the mapping effectively extends beyond the stationary problem and captures the full dissipative evolution toward the NESS. This raises the question of whether the same construction remains valid in the presence of nonlinearity, which is addressed in the next section.

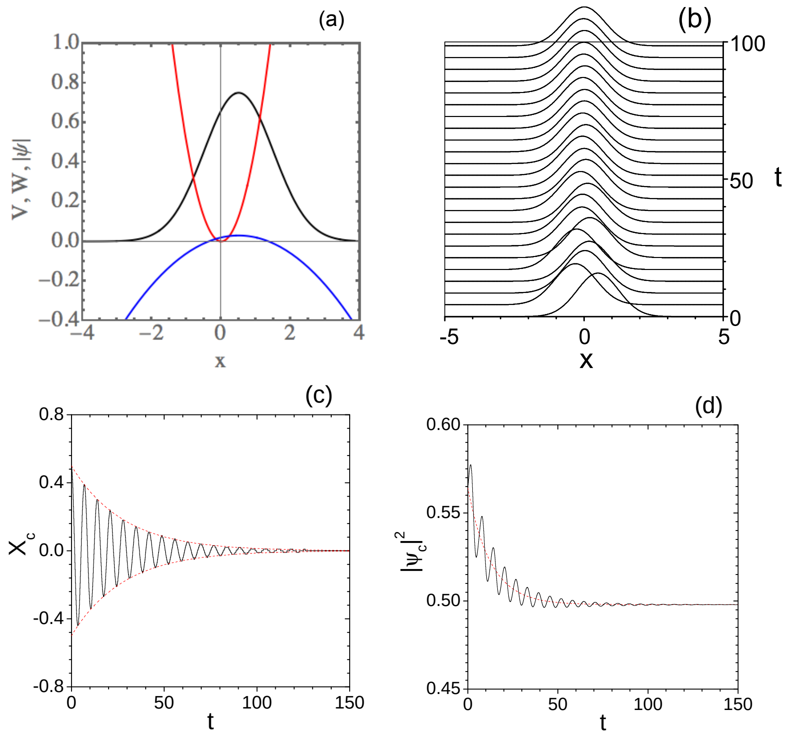

Figure 1. (**a**) Real (red line) and imaginary (blue line) parts of the potential in Equations (20), (22), and ground state wavefunction (black curve) of the displaced harmonic oscillator for parameters $\omega_0 = 1.0, x_0 = 0.5, a_1 = a_2 = -0.02$. (**b**) Time evolution of the density $|\psi(x,t)|^2$ for the initial state in (**a**). (**c**) Damped oscillations of the center of mass versus time. The dashed red curves indicate the fit $x_c(t) \approx \pm x_0 e^{-\xi_c t}$ with $\xi_c \approx 0.036$. (**d**) Peak density amplitude versus time during NESS relaxation (the red curve corresponds to Equation (25)).

4. Nonlinear Dissipative Dynamics

We now investigate the nonlinear regime ($\sigma \neq 0$), using the same complex potential and initial conditions adopted in the linear case. This choice allows for a direct comparison and provides a stringent test of the mapping when applied to time-dependent nonlinear dynamics. The results are summarized in Figures 2 and 3.

Figure 2 compares the time evolution of the center of mass and the peak amplitude for $\sigma = 0, \pm 1$. The left panel shows that, during the transient stage, the nonlinear dynamics closely follows the linear one: the wave packet undergoes damped oscillations toward the trap center with essentially the same decay rate. This indicates that the dissipative mechanism is primarily governed by the engineered complex potential, while nonlinear effects remain comparatively weak during the approach to the trap center.

The right panel of Figure 2 reveals that at $t \approx 100$, immediately after the dissipative transient, the nonlinear dynamics starts to deviate from the linear behavior. While the linear case reaches a constant peak amplitude corresponding to the formation of a NESS, the repulsive case ($\sigma = 1$) displays a slow decrease of the amplitude, indicating a weak decay process. Conversely, the attractive case ($\sigma = -1$) exhibits a gradual growth of the peak amplitude (note the logarithmic scale in Figure 2), eventually leading to collapse on long timescales, as illustrated in the left panel of Figure 3.

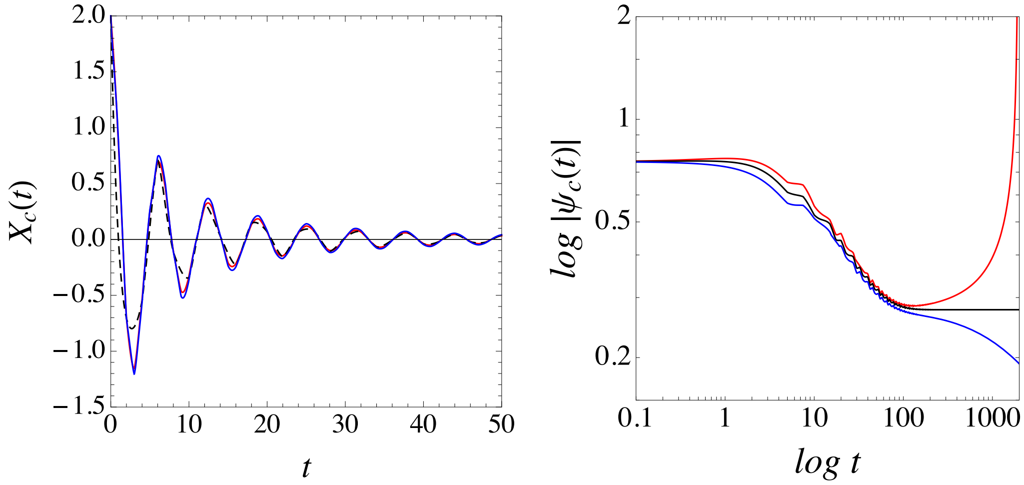

Figure 2. Time evolution of the center of mass (**left panel**) and peak amplitude (**right panel**) for the same complex potential used in the linear case, illustrating the effect of nonlinearity on the dissipative dynamics. The blue and red lines correspond to attractive ($\sigma = -1$) and repulsive ($\sigma = 1$) interactions, respectively, while the black line corresponds to the linear case ($\sigma = 0$) is shown for comparison. The logarithmic scale highlights the slow evolution of the metastable states. Parameters are the same as in Figure 1, except for $x_0 = 2.0$, $a_1 = -0.1$, and $a_2 = -0.1$.

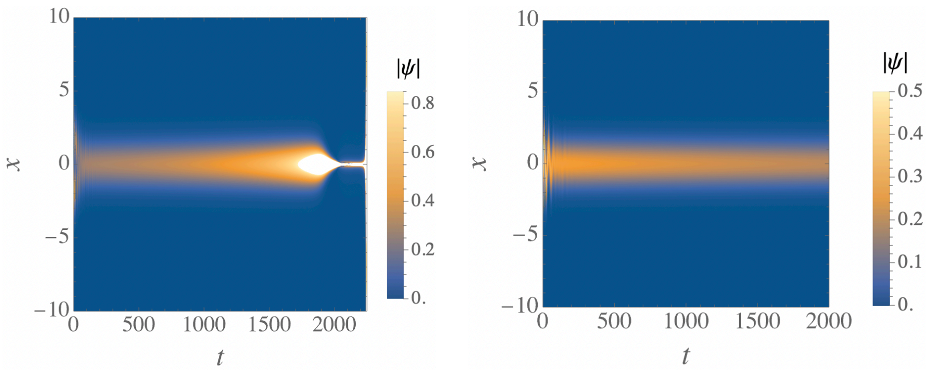

Figure 3. Spatio-temporal evolution of the wave amplitude $|\psi(x,t)|$ in the nonlinear regime for $\sigma = -1$ (**left panel**) and $\sigma = 1$ (**right panel**). The figures show the complete dissipative relaxation toward the trap center during the early stage of the dynamics, followed by the formation of long-lived metastable states. On longer timescales, the attractive case ($\sigma = -1$) undergoes collapse, whereas the repulsive case ($\sigma = 1$) exhibits a slow decay of the wave amplitude. The complex potential and parameter values are the same as in Figure 2.

The formation of metastable states at the trap center is also evident from the spatio-temporal evolution shown in Figure 3. In both attractive and repulsive cases, the system first relaxes toward a quasi-stationary localized state that remains remarkably close to the linear NESS for extended times before the residual instability eventually manifests itself.

This behavior is a direct manifestation of the limitations of the mapping when applied to nonlinear dynamical problems. As discussed in Section 2, the mapping is exact for stationary states, whereas its extension to time-dependent nonlinear evolution should be regarded as a potential-design strategy. Since the nonlinear wave profile gradually departs from the stationary ansatz used to construct the complex potential, the exact gain–loss balance required for perfect NESS formation is no longer maintained, leaving a small residual imbalance at the trap center.

It is remarkable, nevertheless, that the static complex potential design alone is capable of generating metastable states whose lifetimes largely exceed the characteristic dissipative timescale of the transient dynamics in both attractive and repulsive regimes. In the next section, we show that these residual long-term instabilities can be efficiently suppressed by means of nonlinear management, leading to the stabilization of the NESS.

5. Nonlinear Management and NESS Stabilization

The fact that the residual imbalance, unavoidable within a static potential design, depends on the sign of the nonlinearity naturally suggests a route toward NESS stabilization through time-periodic modulation of the interaction strength [8,32].

NM has been extensively investigated as a tool for controlling collapse in attractive multidimensional nonlinear systems [29,33]. However, to our knowledge, its application to the stabilization of non-equilibrium stationary states in nonlinear open systems has received much less attention [34,35]. We stress that the collapse and decay processes displayed in Figure 3 are not related to dimensionality effects, but rather originate from the residual mismatch between gain, loss, and nonlinear interactions that remains in the static potential design. A temporal modulation of the nonlinearity can therefore provide an additional dynamical mechanism capable of compensating for this imbalance and stabilizing the NESS.

To test this idea, we introduce the NM protocol

$$\sigma(t) = \begin{cases} \sigma_0, & t \leq t_0, \\ \sigma_0 \left(1 - \gamma + \frac{\gamma}{2}\left[1 + \cos(\Omega(t - t_0))\right]\right), & t > t_0, \end{cases} \tag{26}$$

where $\sigma_0 = \pm 1$, t_0 denotes the activation time, Ω is the modulation frequency, and γ controls the modulation amplitude. The management is activated after the damped oscillatory stage, when the wave packet has already approached the trap center and the metastable regime is formed.

The results are summarized in Figure 4, where we report the time evolution of the peak amplitude for different values of γ in both the attractive and repulsive cases. As γ increases within the interval $0 \leq \gamma \leq 2$, the amplitude growth observed in the attractive case is progressively suppressed until, at $\gamma = 2$, the state becomes effectively stationary. A similar stabilization against decay occurs in the repulsive case.

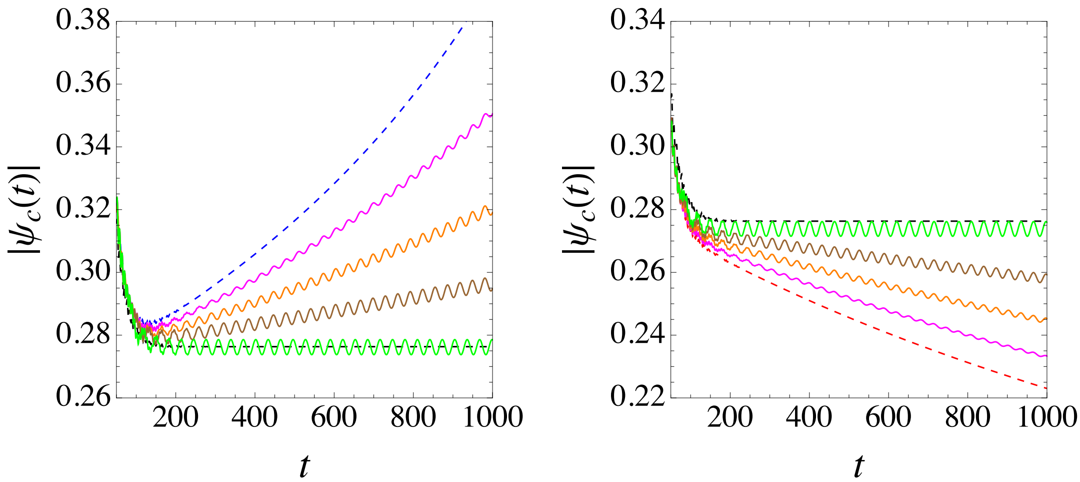

Figure 4. Time evolution of the peak amplitude for attractive, $\sigma_0 = -1$ (**left panel**), and repulsive, $\sigma_0 = 1$ (**right panel**) in the presence of NM nonlinear (continuous curves) with different values of γ. The continuous curves, with magenta, orange, brown, green, colors correspond in both panels to the amplitudes $\gamma = 0.5, 1.0, 1.5, 2.0$, respectively. The dashed blue, black, and red lines refer to the value $\gamma = 0$ (i.e., absence of NM) and coincide with the curves of the same color in the right panel of Figure 2, here plotted in linear scale. The modulation frequency is $\Omega = 0.2$ and the activation times are $t_0 = 100$ and $t_0 = 80$ for left and right panels, respectively. All other parameters are the same as in Figure 2.

Remarkably, in both cases the stabilized NESS is obtained when the nonlinearity oscillates between ± 1, corresponding to a vanishing time-averaged interaction. In this regime, the average peak amplitude becomes very close to that of the linear NESS discussed in Section 3. This indicates that the modulation dynamically compensates for the residual nonlinear imbalance responsible for the slow collapse or decay observed in the unmanaged dynamics.

The modulation frequency used in Figure 4 is intentionally chosen sufficiently small to make the residual oscillations visible. We have verified that increasing Ω, while keeping all other parameters fixed, does not modify the average stabilization dynamics. The only observable effect is the expected reduction of the oscillation period, leading to progressively denser residual oscillations. This demonstrates that the stabilization mechanism is robust over a broad range of modulation frequencies.

We also note that stabilization does not require the limiting case $\gamma = 2$. A broad interval $0 < \gamma < 2$ already produces a substantial increase of the metastable lifetime, effectively pushing the onset of collapse or decay beyond experimentally relevant time scales.

The effectiveness of the NM protocol is further illustrated in Figure 5, where the spatio-temporal evolution of the wave amplitude is reported for the same cases shown in Figure 4, but with the NM protocol of amplitude

$\gamma = 2$ activated. In both attractive and repulsive cases, the metastable configuration evolves into a robust NESS characterized by a nearly stationary localized profile and a dynamically sustained balance between gain, loss, and nonlinear interactions.

The physical mechanism underlying this stabilization can be intuitively understood directly from the nonlinear dynamics preceding the activation of the management protocol. As shown in the right panel of Figure 2, the attractive and repulsive cases evolve almost identically during the dissipative transient and begin to diverge only after the wave has reached the trap center. The attractive interaction then induces a slow increase of the peak amplitude, whereas the repulsive interaction produces a slow decrease. By periodically alternating the sign of the nonlinearity, NM continuously compensates these opposite tendencies over successive modulation cycles, thereby suppressing the residual gain–loss imbalance responsible for the long-term instability. As a result, the metastable configuration is transformed into a genuine non-equilibrium stationary state.

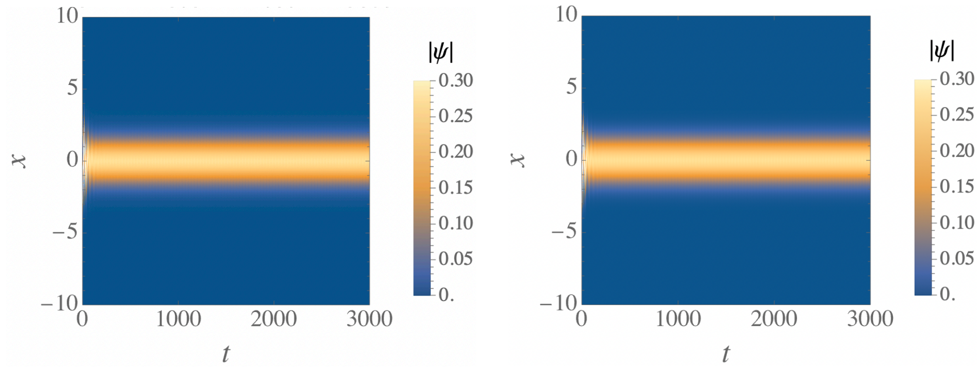

Figure 5. Spatio-temporal evolution of the wave amplitude $|\psi(x,t)|$ in the presence of the NM protocol in Equation (26) with $\gamma = -2$ and $\sigma_0 = -1$, $t_0 = 100$ (**left panel**), $\sigma = 1$, $t_0 = 75$ (**right panel**). All other parameters are fixed as in Figure 3.

6. Conclusions and Experimental Perspectives

In this work, we have investigated the dissipative dynamics of linear and nonlinear waves in harmonic traps using engineered complex non-Hermitian potentials. By exploiting a mapping between real and complex Schrödinger equations, we have shown that it is possible to design complex potentials that induce controlled damping toward the trap center.

In the linear regime, we have shown that the mapping-derived complex potential drives an initially displaced wave packet through damped oscillations toward a NESS localized at the trap center. This demonstrates that engineered complex potentials provide a systematic framework for realizing dissipative quantum oscillators within the context of a non-Hermitian Schrödinger equation.

In the nonlinear regime, the same engineered potential governs the transient dynamics, which closely follows the linear case. The long-time behavior, however, is fundamentally different. Instead of converging to a true stationary state, the system evolves toward a long-lived metastable configuration, reflecting the residual gain–loss imbalance that remains under a static potential design. This imbalance leads to slow decay in the repulsive case and gradual focusing culminating in collapse in the attractive one. We have shown that nonlinear management compensates for this residual mismatch by dynamically modulating the interaction strength, thereby transforming the metastable state into a robust NESS. These results highlight the importance of active dynamical control in nonlinear non-Hermitian systems.

From an experimental perspective, the proposed scenario is directly accessible in both photonic and atomic systems. In nonlinear optics, the real and imaginary parts of the potential can be implemented through refractive-index engineering combined with spatially tailored optical gain and absorption profiles, while Kerr nonlinearities provide access to the interacting regime. In Bose–Einstein condensates, harmonic confinement is naturally available, and the required complex landscapes can be implemented through localized atom removal by focused electron beams or resonant optical beams, together with appropriate feeding techniques, whereas the interaction strength remains finely tunable via Feshbach resonances.

A key advantage of the proposed framework is that the same engineered complex potential can be employed to investigate both the linear and nonlinear regimes without modification. This enables a direct comparison between exact dissipative stabilization and metastable nonlinear dynamics. In particular, the long-lived localized states observed in the nonlinear regime, together with their slow decay or focusing signatures and their full stabilization via NM, represent a robust experimental hallmark of the interplay between nonlinearity and non-Hermiticity.

Funding

The author acknowledges financial support from the University of Salerno and the Department of Physics "E. R. Caianiello" through the local research contracts FARB-2024 and FARB-2025.

Institutional Review Board Statement

Not applicable.

Informed Consent Statement

Not applicable.

Data Availability Statement

Not applicable.

Conflicts of Interest

The author declares no conflict of interest.

Given the role as a member of Editorial Board, the author had no involvement in the peer review of this paper and had no access to information regarding its peer-review process. Full responsibility for the editorial process of this paper was delegated to another editor of the journal.

Use of AI and AI-Assisted Technologies

No AI tool was used for the conception of the research, formulation of the theoretical model, scientific analysis, developing of numerical codes, numerical results, interpretations, and development of conclusions. ChatGPT has been used for purely editorial/language assistance on the text written by the author.

References

1. Aranson, I.S.; Kramer, L. The world of the complex Ginzburg-Landau equation. *Rev. Mod. Phys.* **2002**, *74*, 99–143. https://doi.org/10.1103/revmodphys.74.99.
2. Akhmediev, N.; Ankiewicz, A. (Eds.) *Dissipative Solitons: From Optics to Biology and Medicine*; Springer: Berlin, Heidelberg, Germany, 2008. https://doi.org/10.1007/978-3-540-78217-9.
3. Kivshar, Y.S.; Agrawal, G.P. *Optical Solitons: From Fibers to Photonic Crystals*; Academic Press: San Diego, CA, USA, 2003.
4. Lugiato, L.; Prati, F.; Brambilla, M. *Nonlinear Optical Systems*; Cambridge University Press: Cambridge, UK, 2015.
5. Breuer, H.P.; Petruccione, F. *The Theory of Open Quantum Systems*; Oxford University Press: Oxford, UK, 2002.
6. Rotter, I. A non-Hermitian Hamilton operator and the physics of open quantum systems. *J. Phys. A Math. Theor.* **2009**, *42*, 153001. https://doi.org/10.1088/1751-8113/42/15/153001.
7. Grynberg, G.; Robilliard, C. Cold atoms in dissipative optical lattices. *Phys. Rep.* **2001**, *355*, 335–451. https://doi.org/10.1016/s0370-1573(01)00017-5.
8. Malomed, B.A. *Soliton Management in Periodic Systems*; Springer: New York, NY, USA, 2006. https://doi.org/10.1007/0-387-29334-5.
9. Brazhnyi, V.A.; Konotop, V.V. Theory of nonlinear matter waves in optical lattices. *Mod. Phys. Lett. B* **2004**, *18*, 627–651. https://doi.org/10.1142/s0217984904007190.
10. Morsch, O.; Oberthaler, M. Dynamics of Bose-Einstein condensates in optical lattices. *Rev. Mod. Phys.* **2006**, *78*, 179–215. https://doi.org/10.1103/revmodphys.78.179.
11. El-Ganainy, R.; Makris, K.G.; Khajavikhan, M.; et al. Non-Hermitian physics and $\mathcal{PT}$-symmetry. *Nat. Phys.* **2018**, *14*, 11–19. https://doi.org/10.1038/nphys4323.
12. Feng, L.; El-Ganainy, R.; Ge, L. Non-Hermitian photonics based on parity–time symmetry. *Nat. Photonics* **2017**, *11*, 752–762. https://doi.org/10.1038/s41566-017-0031-1.
13. Bender, C.M.; Boettcher, S. Real spectra in non-Hermitian Hamiltonians having $\mathcal{PT}$-symmetry. *Phys. Rev. Lett.* **1998**, *80*, 5243–5246. https://doi.org/10.1103/physrevlett.80.5243.
14. Bender, C.M. Making sense of non-Hermitian Hamiltonians. *Rep. Prog. Phys.* **2007**, *70*, 947–1018. https://doi.org/10.1088/0034-4885/70/6/r03.
15. Konotop, V.V.; Yang, J.; Zezyulin, D.A. Nonlinear waves in $\mathcal{PT}$-symmetric systems. *Rev. Mod. Phys.* **2016**, *88*, 035002. https://doi.org/10.1103/revmodphys.88.035002.
16. Longhi, S. Bloch oscillations in complex crystals with $\mathcal{PT}$-symmetry. *Phys. Rev. Lett.* **2009**, *103*, 123601. https://doi.org/10.1103/physrevlett.103.123601.

17. Guo, A.; Salamo, G.J.; Duchesne, D.; et al. Observation of $\mathcal{PT}$-symmetry breaking in complex optical potentials. *Phys. Rev. Lett.* **2009**, *103*, 093902. https://doi.org/10.1103/physrevlett.103.093902.
18. Rüter, C.E.; Makris, K.G.; El-Ganainy, R.; et al. Observation of parity–time symmetry in optics. *Nat. Phys.* **2010**, *6*, 192–195. https://doi.org/10.1038/nphys1515.
19. Miri, M.A.; Alù, A. Exceptional points in optics and photonics. *Science* **2019**, *363*, eaar7709. https://doi.org/10.1126/science.aar7709.
20. Musslimani, Z.H.; Makris, K.G.; El-Ganainy, R.; et al. Optical solitons in $\mathcal{PT}$-periodic potentials. *Phys. Rev. Lett.* **2008**, *100*, 030402. https://doi.org/10.1103/physrevlett.100.030402.
21. Abdullaev, F.K.; Konotop, V.V.; Salerno, M.; et al. Dissipative periodic waves, solitons, and breathers of the nonlinear Schrödinger equation with complex potentials. *Phys. Rev. E* **2010**, *82*, 056606. https://doi.org/10.1103/physreve.82.056606.
22. Zezyulin, D.A.; Konotop, V.V. Nonlinear modes in finite-dimensional $\mathcal{PT}$-symmetric systems. *Phys. Rev. Lett.* **2012**, *108*, 213906. https://doi.org/10.1103/physrevlett.108.213906.
23. Konotop, V.V.; Yang, J.; Zezyulin, D.A. Nonlinear waves in $\mathcal{PT}$-symmetric systems. *Rev. Mod. Phys.* **2016**, *88*, 035002. https://doi.org/10.1103/revmodphys.88.035002.
24. Li, K.; Cai, Y.; Yan, J.; et al. Direct manipulation of biphoton generation from the non-Hermitian nature of light-matter interaction. *Laser Photonics Rev.* **2025**, *19*, 2402149. https://doi.org/10.1002/lpor.202402149.
25. Chen, Q.; Zhuang, R.; Tang, H.; et al. Non-Hermitian jumps and EP loops in the rates of coincidence counts of time-energy-entangled W triphotons. *Adv. Quantum Technol.* **2026**, *9*, e70323. https://doi.org/10.1002/qute.70323.
26. Graefe, E.M. Stationary states of a $\mathcal{PT}$-symmetric two-mode Bose–Einstein condensate. *J. Phys. A Math. Theor.* **2012**, *45*, 444015. https://doi.org/10.1088/1751-8113/45/44/444015.
27. Salerno, M. Mapping between nonlinear Schrödinger equations with real and complex potentials. *J. Geom. Symm. Phys.* **2013**, *32*, 25–35. https://doi.org/10.7546/jgsp-32-2013-25-35.
28. Prosen, T. Open XXZ spin chain: Nonequilibrium steady state and a strict bound on ballistic transport. *Phys. Rev. Lett.* **2011**, *106*, 217206. https://doi.org/10.1103/physrevlett.106.217206.
29. Abdullaev, F.K.; Caputo, J.G.; Kraenkel, R.A.; et al. Controlling collapse in Bose-Einstein condensates by temporal modulation of the scattering length. *Phys. Rev. A* **2003**, *67*, 013605. https://doi.org/10.1103/physreva.67.013605.
30. Pitaevskii, L.; Stringari, S. *Bose-Einstein Condensation and Superfluidity*; Oxford University Press: Oxford, UK, 2016.
31. Salerno, M. Macroscopic quantum bound states and Josephson effect in Bose-Einstein condensates in optical lattices. *Laser Phys.* **2005**, *15*, 620–625.
32. Centurion, M.; Porter, M.A.; Kevrekidis, P.G.; et al. Nonlinearity management in optics: experiment, theory, and simulation. *Phys. Rev. Lett.* **2006**, *97*, 033903. https://doi.org/10.1103/physrevlett.97.033903.
33. Sakaguchi, H.; Malomed, B.A. Resonant nonlinearity management for nonlinear Schrödinger solitons. *Phys. Rev. E* **2004**, *70*, 066613. https://doi.org/10.1103/PhysRevE.70.066613.
34. Diehl, S.; Micheli, A.; Kantian, A.; et al. Quantum states and phases in driven open quantum systems with cold atoms. *Nat. Phys.* **2008**, *4*, 878–883. https://doi.org/10.1038/nphys1073.
35. Popkov, V.; Salerno, M. Dissipative cooling towards phantom Bethe states in boundary-driven XXZ spin chain. *Europhys. Lett.* **2022**, *140*, 11004. https://doi.org/10.1209/0295-5075/ac954b.